

Differential rotation within the Earth's outer core

Raymond Hide^{1,2}, Dale H. Boggs¹, Jean O. Dickey¹

¹Jet Propulsion Laboratory, California Institute of Technology, 4800 Oak Grove Drive, Pasadena, CA 91109-8099, USA

²Physics Department (Atmospheric, Oceanic and Planetary Physics), Oxford University, Clarendon Laboratory, Parks Road, Oxford OX2 3PU, England, UK

Non-steady differential rotation drive by buoyancy forces within the Earth's liquid outer core (OC) plays a key rôle not only in the generation of the main geomagnetic field by the magnetohydrodynamic (MHD) dynamo process but also in the excitation of irregular fluctuations in the angular speed of rotation of the overlying solid mantle, as evinced by changes in the length of the day (LOD) on decadal and longer timescales (1-8). Its broad characteristics are investigated by dividing the core into a number of imaginary equivolume cylindrical annuli coaxial with the axis of rotation of the Earth and determining temporal fluctuations in the axial component of angular momentum of each annulus under simplifying assumptions about the flow at depth within the core. Using available velocity fields just below the core-mantle boundary (CMB) based on geomagnetic secular variation (GSV) observations, we investigate core angular momentum (CAM) fluctuations over fifteen decades from 1840–1990 and find the dominant mode of variability to be ~65 years. This timescale is consistent with those found in earlier analyses of LOD and GSV timeseries by Vestine, Stoyko, Orly, Currie, Kahle, Yukutake and others (1, 2, 9), which could, according to Braginsky (9), be the fundamental period of torsional MHD oscillations of the core if lines of force of the poloidal part of the magnetic

field there are strongly aligned with the rotation axis, as in his “model Z” dynamo (10, 12). The mid-latitude CAM fluctuations are generally out of phase with fluctuations found in equatorial regions, but significantly they are roughly in phase with LOD fluctuations. The largest positive correlation (0.8 when data before 1867.5 are excluded) are observed in the mid-latitudes with the main maxima at zero lag with secondary peaks being consistent with a 65-year periodicity. Propagation of CAM anomalies from the equatorial to polar regions is also revealed by the analysis.

Fluctuating motions including differential rotation in the OC are driven by buoyancy forces due to the action of gravity on density inhomogeneities associated with differential heating and cooling. They are strongly influenced by Coriolis forces due to the Earth’s rotation, which render the motions sensitive to the geometry and lateral variations in physical properties of the bounding surfaces, and also by Lorentz forces due to the presence of electric currents within the core which, except in the outer reaches of the core (13), may be comparable in magnitude with Coriolis forces (14). The present study is a further step toward the elucidation of the dynamical processes within the Earth’s deep interior that give rise to decadal fluctuations in the rate of rotation of the solid Earth and involve angular momentum transfer not only between the core and the overlying mantle but also between different parts of the core.

Considerations of differential rotation and associated fluctuations in angular momentum and of the exchange of angular momentum between the fluid and the regions with which it is in contact are of fundamental importance in dynamical studies of any geophysical or astrophysical spinning fluid system. Strong indirect evidence of angular momentum exchange between the OC and the overlying mantle came initially from general quantitative considerations made in the first realistic attempts to interpret determinations of LOD fluctuations on decadal time scales. The LOD is an inverse measure of the axial component of angular momentum of the main part of the solid Earth,

namely the mantle, crust and cryosphere, and it has long been generally accepted that irregular LOD fluctuations on such time scales must be due largely to core motions (4).

It is the comparatively high moment of inertia of the OC, more than 10^5 times that of the atmosphere, that makes it possible for slow motions within it to produce effects on the rotation of the solid Earth that are larger than meteorological effects, but which occur on longer timescales. Thus, the amplitude of sub-decadal LOD fluctuations excited by the atmosphere is typically about a millisecond (ms), while decadal LOD fluctuations excited by the core can be as large as 5 ms (4). At a fraction of a millimeter per second, the speed of core motions is typically no more than 10^{-4} times that of atmospheric winds: one week for the atmosphere thus translates into about a century for the core, so the 150 years of geomagnetic data available for the present study can provide no more than a glimpse of what might be happening in the core. Work on the interpretation of sub-decadal LOD fluctuations in terms of dynamical processes in the atmosphere is now well advanced owing, in large part, to the abundance of meteorological data. Characteristic timescales of the relevant meteorological phenomena are generally much shorter than the data span, so that data analyses are robust and detailed investigations of angular momentum transfer between different parts of the atmosphere and between the atmosphere and the underlying planet are feasible. The present study of CAM fluctuations is comparatively limited in both temporal and spatial resolution, but it is the best that can be accomplished with available GSV and LOD data.

It is impossible in this short letter to refer to all the relevant literature, which goes back several decades, but extensive bibliographies listing much original work can be found in many of the references cited. The findings of the present study complement and are generally consistent with recent independent analyses of GSV and LOD data along related but different lines reported in references 10 and 11.

If $M_S(t)$ is the axial component of the angular momentum of the solid Earth and $M(t)$ that of the liquid core, on decadal time scales the equation

$$\dot{M} + \dot{M}_s = 0 \quad (1)$$

(where t denotes time and $\dot{M} = dM/dt$, etc.) expresses angular momentum conservation to better than 10% (the residual being largely associated with atmospheric and oceanic effects). M is given by the axial component of

$$\iiint \rho(\mathbf{r}, t) \mathbf{r} \times [\boldsymbol{\Omega} \times \mathbf{r} + \mathbf{u}] d\tau \quad (2)$$

where $\rho(\mathbf{r}, t)$ is the mass density at a general point P in a frame of reference with its origin at the Earth's centre of mass and which rotates with the mantle with angular velocity $\boldsymbol{\Omega}$ relative to an inertial frame and \mathbf{u} is the Eulerian relative flow velocity, and $d\tau$ is an element of volume of the liquid core, over the whole of which the volume integral is taken.

To conserve the angular momentum of the whole system, any fluctuations in M must be accompanied by fluctuations in the angular momentum not only of the overlying solid mantle but also of the underlying solid inner core which, being a good electrical conductor, should be tightly coupled by Lorentz forces to the OC. However, in comparison with the OC, the volume of the solid inner core is small, no more than 4 percent of the total volume of the core in the present study (see Figure 1), and its moment of inertia is even smaller in comparison, much less than 1% of that of the OC. Given the accuracy level of angular momentum budget analyses, any contributions to \dot{M}_s associated with possible fluctuations in the motion of the inner core can be neglected in the calculations presented here. Further justification for this assumption is implied by seismological and other important new work (reported after the present study was completed) of the relative rotation of the inner core (15, 16).

Fig. 1 near here

Table 1 near here

The LOD data used comprise a self-consistent time-series resulting from the analyses of lunar occultations prior to 1955.5 and then a combination of astronomical and modern geodetic techniques are utilized (17). Solar eclipses and other data (18) indicate that the LOD has increased over the past 2700 years at an average rate of at 1.70 ± 0.05 ms/cy, largely attributable to tidal braking of the Earth's spin (2.3 ± 0.1 ms/cy) and changes in the Earth's polar moment of inertia associated with "post-glacial rebound" (-0.6 ± 0.1 ms/cy). This trend of 1.7 ms/cy was removed from the LOD series before comparing it with CAM fluctuations.

Just as it is customary to divide the atmosphere into the troposphere, stratosphere and higher regions, and the oceans into the thermocline and lower regions, it is convenient to divide the OC into the "torosphere" and "polosphere" (19). Within the former the toroidal magnetic field is so strong that Lorentz forces are comparable in magnitude with Coriolis forces (14). Within the overlying "polosphere," where the toroidal magnetic field is typically no stronger than the poloidal field, Lorentz forces are correspondingly much weaker than Coriolis forces (13). Owing to the presence of the solid inner core, Coriolis forces inhibit flow across the imaginary cylindrical surface that is tangential to the inner core at the equator and intersects the outer core at latitudes $\pm 66^\circ$ (see Figure 1), so it is convenient to subdivide the liquid core further into "polar" regions lying within the tangent cylinder and "extrapolar" regions lying outside the cylinder (14). This scheme proves useful not only in work on the dynamics of the Earth's core but also in studies of other geophysical and astrophysical fluids, such as the various fluid layers of Jupiter and Saturn and the convective outer layers of the Sun. Some justification for the scheme came initially from laboratory experiments by one of us (RH) on thermal convection in an electrically-insulating rotating spherical fluid annulus upon which the scheme was originally based, and further justification is provided by the flow fields

produced in numerical models of buoyancy-driven MHD flows in the Earth's core (20). It may be significant in connection with the interpretations of the findings of this paper that motions can be more vigorous in midlatitudes than elsewhere.

We suppose here that the Earth's liquid metallic outer core is bounded by concentric spherical surfaces of radii $c = 3485$ km and $b = 1222$ km (see Figure 1 and Table 1) and we divide the core into $Q = 20$ cylindrical annuli of equal volume. These choices of equivolume annuli and of 20 for the total number, Q , were arbitrary but convenient. They facilitated calculations without affecting the main findings of the investigation. Solutions with fewer ($Q = 10$) and more ($Q = 40$) annuli indicate that these findings are robust and insensitive to the choice of Q over a wide range. The total axial angular momentum $\mu_q(t;Q)$ of the q -th cylindrical annulus associated with relative core motions with Eulerian flow velocity $\mathbf{u}(\mathbf{r}, t) = (u, v, w)$ at a general point P with spherical polar coordinates (r, θ, ϕ) is given by

$$\mu_q(t;Q) \equiv \frac{4\pi}{3Q} (c^3 - b^3) \{\rho w r \sin \theta\}_q. \quad (3)$$

Here $\rho = \rho(r, \theta, \phi, t)$ is the density at P , $w = w(r, \theta, \phi, t)$ and the symbol $\{\}_q$ denotes the spatial average over the volume occupied by the q -th annulus (see Figure 1).

Owing to the inaccessibility of the core, direct determinations of $\mathbf{u}(\mathbf{r}, t)$ and $\rho(\mathbf{r}, t)$ are impossible, but methods have now been developed for making indirect estimates of the (θ, ϕ) components (v_s, w_s) of \mathbf{u}_s , the Eulerian flow velocity just below the CMB, where $r \doteq c$, from geomagnetic secular variation data (for excellent review of extensive literature see reference 21). The data used in the present study cover the interval from 1840 to 1990 and were kindly provided by Dr. Andrew Jackson. By supposing for simplicity that axial variations in ρw in the direction parallel to the rotation axis are negligibly small on average, ρw can be replaced in Eq. (3) by the known quantity

$$\frac{1}{2}\bar{\rho}[w_s(\theta, \phi, t) + w_s(\pi - \theta, \phi, t)]. \quad (4)$$

With this key assumption (5) linking the flow just below the CMB to that at depth within the core, we obtain the following approximate relationship for $\mu_q(t; Q)$:

$$\mu_q(t; Q) = \frac{2\pi\rho_s c(c^3 - b^3)}{3Q} \langle [w_s(\theta, \phi, t) + w_s(\pi - \theta, \phi, t)] \sin \theta \rangle_q. \quad (5)$$

Here $\langle \rangle_q$ signifies the spatial average over the surface area of the q -th annulus, covering the ranges $0 \leq \phi \leq 2\pi$ and $\theta_{q-1} \leq \theta \leq \theta_q$. The quantity

$$M(t) = \sum_{q=1}^p \mu_q(t; Q), \quad (6)$$

(see Eq. (5) and (2)) is thus an approximate measure of the total axial angular momentum associated with relative motions in the core.

The assumption that the longitudinally-averaged value of ρw is effectively the same in all planes perpendicular to the axis of rotation provides the simplest (but admittedly approximate) imaginable basis for estimating angular momentum fluctuations in the core from determinations of \mathbf{u} at one level, just below the CMB. It is noteworthy in this connection that previous use of this assumption, by Jault *et al.* (5) and by Jackson *et al.* (7) in investigations of fluctuations in M , the total angular momentum of the OC (see Eq. 6), for comparison with decadal fluctuations in M_s from LOD observations gives remarkably consistent results. By Proudman's celebrated theorem supported by a variety of theoretical and laboratory studies of mechanically-driven flows in rapidly spinning fluids the assumption would hold with great accuracy nearly everywhere when the fluid is homogeneous in density (and electrically-insulating) (22). But the assumption becomes

less reliable when, as in the case of buoyancy-driven flows, density inhomogeneities are present (23), and further complications are associated with Lorentz forces due to the presence of electric currents (1, 23, 24). Thermal convection in rotating fluid spheres (25) and spherical annuli is certainly rendered highly anisotropic by gyroscopic (Coriolis) forces, which tend to align fluid eddies with the main rotation axis of the system. In the geodynamo it is this gyroscopic alignment of fluid eddies in the core (26) that most likely accounts for the link between the Earth's magnetic and rotation axes, upon which of course the principle of the magnetic compass is based.

The total core angular momentum $M(t)$ as well as the contributions from the individual annuli $\mu_q(t; 20)$ are displayed in Fig. 2(a). Here we introduce the "equivalent millisecond unit" (emsu), defined as that amount of axial angular momentum, namely $0.60 \times 10^{26} \text{ kg m}^2\text{s}^{-1}$, which, if transferred to the overlying solid Earth would (if the solid Earth were perfectly rigid) reduce the length of the day (LOD) by 1 ms. Two broad maxima occur in $M(t)$ with the highest value attained around 1900 with "full width half max" (FWHM) of ~25 years (Fig. 2a). The other, smaller, maximum has its peak near 1970 with FWHM of 15 years. A substantial range of variability is exhibited by individual annuli [Fig. 2(b)], with time-averaged total CAM, \bar{M} (say), being negative (-0.237 emsu). The equatorial annulus ($q = 20$), with the largest lever arm, produces the largest (in magnitude) contribution to $M(t)$, with largely negative time-averaged values (i.e., $\mu_{20} \approx -0.4$ emsu). The two large peaks are clearly seen in the annuli with $q = 18-20$ (Fig. 2a); the first peak near 1885 corresponds to the plateau region near 1885 in M , the total CAM, and the second peak occurs near the 1975 maximum in total CAM. The other bands are also highly bimodal, with annuli $q = 16-19$ having their maxima near 1885 and 1950, while annuli 3-15 have maxima near 1910 and 1970. The contribution from annuli $q = 1-3$, with short lever arms, are comparatively small, with the largest contribution occurring around 1910.

Figs. 2-6 near here

Table 2 near here

The three dimensional diagram (Fig. 3) of the contributions μ_q from the individual annuli given as a function of time provides unique insight into core dynamics. The dominant feature is a strong ~ 65 year oscillation which is particularly evident in the midlatitude annuli $q = 3-15$. It might be significant that the maxima in the midlatitude coincide in time with the largest of the so-called geomagnetic “jerks” seen in GSV data (1) over the time period considered, namely, epochs 1912 and 1969. Variability in annuli $q = 16-20$ generally precedes that in the midlatitudes, with results suggestive of angular momentum propagation from the equatorial toward midlatitude regions. On the basis of Figs. 1–3 and Table 2, we divide the core into three regions: polar (P), midlatitude (ML) and equatorial (EQ). The polar region (where $q = 1-3$) is a natural division given the dimension of the solid inner core (Fig. 1), whereas the empirical subdivision into midlatitude ($q = 4-15$) and equatorial ($q = 16-20$) regions is motivated by the characteristic behavior of these two regions. The comparison of LOD fluctuations with total CAM fluctuations (Fig. 4) shows that, in agreement with previous work (5, 7), the decadal LOD variability is well matched with $M(t)$, especially after 1870. Data prior to 1870 are less reliable than more recent data, with a mismatch in the series occurring during the series between 1840–1870. The maximum correlation between $M(t)$ and LOD (Table 1) is 0.58 at a lag of ~ 17.5 yrs when the full series (1840–1990) is considered. It rises to 0.64 when a lag of ~ 5 yrs when the shorter series (1870–1990) is considered. The $M(t)$ data spacing is 2.5 yrs, so an apparent lag of 5 years might not be statistically significant.

The contribution from midlatitudes (\dot{M}_{ML}) (Fig. 3 and 4) dominates \dot{M} and accounts for a major portion of the LOD decadal variability (56.9% for the full series and 74.9% for the short series). M_{ML} is in phase with LOD, having a maximum correlation of 0.8 with the shorter series and 0.5 for the full series (Fig. 5); secondary maxima occur at 67 and -64 years, consistent with a periodicity of approximately 65 years.

The equatorial CAM (M_{EQ} ; annuli $q = 16-20$) time series is bimodal, with maxima at 1885 and 1950, and leads the M_{ML} by ~ 20 years (Fig. 4). The correlation of M_{EQ} with LOD has a principal maximum at a lead of ~ 25 years with secondary maxima near 44 and 90 years, again consistent with a 65-year periodicity. It is the superposition of these two groups of annuli (ML and EQ) that gives rise to the broad CAM maximum near 1900.

The correlation of individual annuli with LOD (Fig. 6) suggests that angular momentum anomalies propagate from the equatorial to the polar annuli. The total CAM, M (see Equation 6) exhibits a principal maximum at a 15-year lead with respect to LOD and secondary maxima at an 80-year lead and at a 60-year lag (note the ~ 65 -year periodicity). The diagram clearly displays the ~ 65 -year period with 4 maxima visible (two strong, two weak) and 4 minima. The strong propagation pattern indicates that the signal takes about 60 years to move from the equatorial regions to the polar regions. Similarly, a propagation pattern is evident in top line plots as the peaks and valleys are traced from one cylinder to another.

In the case of subdecadal Earth rotation fluctuations excited by atmospheric motions, the torques responsible for angular momentum transfer between the Earth's atmosphere and the underlying planet are due to tractions produced by turbulent viscosity in the oceanic and continental boundary layers and also to topographic tractions due to normal pressure forces acting on orography. Topographic torques and boundary layer torques produced by atmospheric motions are typically comparable in magnitude but they have somewhat different temporal characteristics. Much less is known about the torques at the Earth's core-mantle boundary (CMB) that give rise to LOD fluctuations on decadal and larger timescales (4-11, 19). It is generally considered that viscous effects are probably much less important than those due to (a) Lorentz forces associated with electric currents in the lower reaches of the mantle, (b) topographic torques associated with a bumpy core mantle boundary, and (c) gravitational torques. Uncertainties about the

electrical conductivity of the lower mantle and of the shape of the CMB and horizontal density variations in the mantle and core make it difficult at present to establish the relative importance of those agencies. According to one recent study (27) topographic torques are of sufficient magnitude to explain the observed decadal LOD variations, with dominant contributions to the torque arising in midlatitudes, where the most vigorous core motions may occur (see above). This is consistent with our finding that midlatitude CAM fluctuations are in phase with fluctuations in the motion of the mantle.

As to the roughly 65-year period seen in the angular momentum fluctuations presented in Figures 2 and 3, the simplest (but by no means unique) interpretation is to suppose, following Braginsky (9), that it can be identified with the main eigenmode of torsional MHD oscillations with $B_p \doteq 2 \times 10^{-4} T$, where B_p is the average strength of the non-axial component of the poloidal magnetic field in the core. This is about half the average strength of the (poloidal) magnetic field in the lower mantle (1) and no more than about 1% of likely strength of the toroidal part of the magnetic field within the Earth which is effectively confined to the core (1, 14).

Unlike non-axisymmetric MHD oscillations of a spinning fluid (14, 28), purely torsional oscillations about the rotation axis depend only on Lorentz forces associated with the poloidal part of the magnetic field and are unaffected by Lorentz forces associated with the toroidal part of the field and by Coriolis forces. The value of B_p is not known, but it might be as large as $10^{-3} T$. It could however be much smaller if lines of force of the poloidal part of the geomagnetic field are aligned by core motions so that they are almost parallel to the Earth's rotation axis nearly everywhere within the core, as in Braginsky's "model Z" dynamo (12).

As to the excitation of MHD torsional oscillations within the core, the fluctuating background of three-dimensional flow there would be effective if in the power spectrum of the fluctuations there is sufficient energy to overcome attenuation (largely due to ohmic dissipation associated with electric currents induced in the weakly-conducting

lower mantle (1)). It must be emphasized, however, that the 65-year period may turn out to be unrelated to MHD torsional oscillations in the core, and rather reflect the time scale of some dominant instability or nonlinear mode interaction responsible for angular momentum advection within the core. Detailed discussion of excitation and attenuation mechanisms, including the role of advection and other nonlinear processes in the dynamics of torsional oscillations, lies beyond the scope of the present paper. Recently developed numerical models of core flow and the geodynamo (20, 29) might facilitate future research on differential rotation when difficulties associated with the need to use “hyperviscosity” in the models have been overcome (30). Indeed, stringent tests of such models would be their ability to simulate the findings of this investigation of differential rotation of the Earth’s core, based as it is on actual observations of the geomagnetic field and of fluctuations in the Earth’s rotation.

REFERENCES

1. Jacobs, J. A. (ed). *Geomagnetism* (4 vols), London: Academic Press (1987-1991).
2. Jacobs, J. A. *The Earth’s core*, London: Academic Press (1975).
3. Melchior, P. *The physics of the Earth’s core*, Oxford: Pergamon Press (1986).
4. Lambeck, K. *The Earth’s variable rotation*, Cambridge University Press (1980).
5. Jault, D., Gire, C., and Le Mouél, J.-L. Westward drift, core motions and exchange of angular momentum between the core and mantle. *Nature* **333**, 353-356 (1988).
6. Hide, R. and Dickey, J. O. Earth’s variable rotation. *Science* **253**, 629-637 (1991).
7. Jackson, A., Bloxham, J., and Gubbins, D. Time-dependent flow at the core surface and conservation of angular momentum of the coupled core-mantle system. In *Dynamics of Earth’s deep interior and Earth rotation* (ed. J.-L Le Mouél, D. E. Smylie and T. A. Herring), *Geophys. Monog. Amer. Geophys. Un.* **72**, 97-107 (1993).

8. Eubanks, T. M. Variations in the orientation of the Earth. In *Contributions of space geodesy to geodynamics* (ed. D. E. Smith and D. L. Turcotte), Geodynamics Series Vol. 24, *Amer. Geophys. Un.* pages 1-54 (1993).
9. Braginsky, S. I. Torsional magnetohydrodynamic vibrations of the Earth's core and variations in the length of the day. *Geomag. Aeron.* **10**, 3-12 (1970).
10. Zatman, S. and Bloxham, J. Torsional oscillations and the magnetic field within the Earth's core. *Nature* **388**, 760-763 (1997).
11. Jault, D., Hulot, G., and Le Mouél, J-L. Mechanical core-mantle coupling and dynamo modelling. *Phys. Earth Planet. Int.* **98**, 187-191 (1996).
12. Braginsky, S. I. Near axisymmetric models of the hydromagnetic dynamo of the Earth. *Geomag. Aeron.* **15**, 122-128 (1975).
13. LeMouél, J-L. Outer core geostrophic flow and secular variations of Earth's magnetic field. *Nature* **311**, 734-735 (1984).
14. Hide, R. Free hydromagnetic oscillations of the Earth's core and the theory of the geomagnetic secular variation. *Phil. Trans. Roy. Soc.* **A259**, 615-647 (1966).
15. Song, X. and Richards, P. G. Observational evidence for differential rotation of the Earth's inner core. *Nature* **382**, 221-224 (1996).
16. Glatzmaier, G. A., and Roberts, P. H. Rotation and magnetism of the Earth's inner core. *Science* **274**, 1887-1891 (1996).
17. Jordi, C., Morrison, L. V., Rosen, R. D., Salstein, D. A., and Rossello, G. Fluctuations in the Earth's rotation since 1983 from high-resolution astronomical data. *Geophys. J. Intern.* **117**, 811-818 (1994).
18. Stephenson, F. R. and Morrison, L. V. Long-term fluctuation in the Earth's rotation—700 B.C. to A.D. 1990. *Phil. Trans. Roy. Soc. A* **351**, 165-202 (1995).
19. Hide, R. The topographic torque on the rigid bounding surface of a rotating gravitating fluid and the excitation of decadal fluctuations in the Earth's rotation. *Geophys. Res. Lett.* **22**, 961-964 and 3563-3565 (1995).

20. Glatzmaier, G. A. and Roberts, P. H. A three-dimensional convection dynamo with rotating and finitely conducting inner core and mantle. *Phys. Earth Planet Inter.* **91**, 63-75 (1995).
21. Bloxham, J., and Jackson, A. Fluid flow near the surface of the Earth's outer core. *Rev. Geophys.* **29**, 97-120 (1991).
22. Greenspan, H. P. *The theory of rotating fluids*, Cambridge University Press (1968).
23. Hide, R. Hydrodynamics of the Earth's core. *Phys. Chem. Earth* **1**, 94-137 (1956).
24. Taylor, J. B. The magnetohydrodynamics of a rotating fluid and the Earth's dynamo problem. *Proc. Roy. Soc.* **A274**, 274-283 (1963).
25. Boubnov, B. M. and Golitsyn, G. S. *Convection in rotating fluids*. Dordrecht: Kluver (1995).
26. Elsasser, W. M. On the origin of the Earth's magnetic field. *Phys. Rev.* **55**, 489-500 (1939).
27. Hide R., Clayton, R. W., Hager, B. H., Spieth, M. A., and Voorhies, C. V. Topographic core-mantle coupling and fluctuations in the Earth's rotation. In *Relating geophysical structures and processes: The Jeffreys Volume*. (ed. K. Aki and R. Dmowska), *Geophys. Monog. Amer. Geophys. Un.* **76**, 107-120 (1993).
28. Braginsky, S. I. Magnetohydrodynamics of the Earth's core. *Geomag. Aeron.* **4**, 698-712 (1964).
29. Kuang, W. and Bloxham, J. An Earth-like numerical dynamo model. *Nature* **389**, 371-374 (1997).
30. Zhang, K. and Jones, C. A. The effect of hyperviscosity on geodynamo models. *Geophys. Res. Lett.* **24**, 2869-2872 (1997).

Acknowledgements. The velocity data, based on geomagnetic secular variation observations, used in this study were kindly provided by Dr. Andrew Jackson. We also wish to acknowledge helpful discussions and correspondence with David Barraclough,

Danan Dong, Richard Gross, Brad Hager, Jean-Louis LeMouél, Steven Marcus, Leslie Morrison and Paul Roberts. This work presents the findings of one phase of research carried out at the Jet Propulsion Laboratory, California Institute of Technology, sponsored by the National Aeronautics and Space Administration.

Table 1

q	θ_q	q	θ_q	q	θ_q	q	θ_q
1	12.56	6	28.94	11	40.95	16	54.80
2	17.52	7	31.38	12	43.43	17	58.42
3	20.99	8	33.77	13	46.01	18	62.78
4	23.80	9	36.15	14	48.72	19	68.71
5	26.43	10	38.53	15	51.62	20	90.00

Legends for Diagrams and Tables

Figure 1. Illustrating the division of the Earth's liquid outer core into $Q = 20$ cylindrical annuli of equal volume numbered $q = 0, 1, 2, 3 \dots 20$ and bounded on the equatorward side by the co-latitude θ_q in the Northern Hemisphere and $\pi - \theta_q$ in the Southern Hemisphere, where values of θ_q are shown in Table 1.

Figure 2. (a) Temporal fluctuations in $\mu_q(t; Q)$, $q = 0, 1, 2, 3 \dots Q = 20$, the angular momentum of each annulus, from 1840 to 1990 (thin lines) and of $M(t)$, the total angular momentum (thick line) (see Eq. 5 and 6 and Figure 2(b)); (b) the dependence on q of the temporal mean value of $\mu_q(t; Q)$, the core angular momentum, from 1840 to 1980 (thick broken line) and of the range of temporal fluctuations (thin broken lines). For each value of q , the fluctuation shown in Figure 2(a) is about a mean value given in Figure 2(b).

Figure 3. Three-dimensional representation of core angular momentum of 20 co-axial equivolume cylindrical annuli as a function of annulus number, q , and time (Hovmöller diagram). Note the dominant ~65-year fluctuation and its latitude dependence. Related statistical data are given in Table 2.

Figure 4. Comparison of length of day (LOD) and core angular momentum (CAM). A slope of 1.7 ms/century has been removed from the LOD data to allow for the effects of post-glacial rebound and the secular acceleration of the Moon and a 10-year smoothed series are shown from each of the series. The total CAM (M) is shown as well as three regions (annuli $q = 1-3$, $q = 4-15$, $q = 16-20$). Note the large correlation between LOD and midlatitude region (annuli $q = 4-15$).

Figure 5. The correlation of grouped (annuli $q = 1-3$, $q = 4-15$, $q = 16-20$) of CAM with LOD as a function of lag of the CAM with respect to the LOD. The top curve (a) is based on the full series (1840–1990), and the bottom curve (b) on the shorter series (1867.5–1990) where the correlation is higher.

Figure 6. Correlation of LOD (length of day) with the CAM (core angular momentum) as a function of the lag of the CAM with respect to the length of day. The effect of the individual annuli are shown in black and by the color graphics; the total CAM effect is depicted by the red line.

Table 1. Values of θ_q (in degrees) where $q = 0, 1, 2, 3, \dots, Q (= 20)$.

Table 2. Statistical data relating to Figure 3.

CAM _i /CAM _{TOTAL}					CAM _i /LOD			
Belts	Correlation Lag = 0	Max Correlation	Lag (years) at max Correlation	% Variance Explained	Correlation Lag = 0	Maximum Correlation	Lag (years) at max Correlation	% variance Explained
1	.16	.33	15	.2	.20	.22	-2.5	.4
2	.32	.48	12.5	1.6	.32	.36	-2.5	2.5
3	.48	.61	7.5	2.8	.42	.44	-2.5	3.9
4	.62	.74	7.5	3.8	.50	.52	-2.5	5.0
5	.73	.83	7.5	4.8	.55	.58	-2.5	5.8
6	.79	.86	5	5.6	.56	.58	-2.5	6.4
7	.81	.86	5	6.3	.54	.56	-2.5	6.7
8	.81	.83	2.5	6.7	.51	.53	-2.5	6.8
9	.80	.81	2.5	7.0	.47	.49	-2.5	6.6
10	.79	.79	2.5	7.0	.42	.45	-2.5	6.0
11	.78	.78	0	6.8	.38	.41	-5	5.2
12	.79	.79	0	6.4	.32	.40	-10	4.2
13	.81	.81	0	5.9	.25	.41	-12.5	2.9
14	.84	.84	0	5.2	.16	.48	-20	1.4
15	.81	.81	0	4.4	-.02	.61	-20	-.2
16	.66	.66	0	3.7	-.21	.67	-22.5	-1.9
17	.46	.56	-15	3.2	-.33	.66	-25	-3.6
18	.36	.58	-15	3.2	-.37	.65	-25	-5.2
19	.39	.62	-15	4.3	-.36	.67	-25	-6.3
20	.59	.69	-7.5	11.28	-.17	.64	-22.5	-5.4
1-3	.38	.53	10	4.6	.36	.38	-2.5	6.9
4-15	.88	.88	2.5	69.8	.47	.49	-7.5	56.9
16-20	.56	.69	-7.5	25.6	-.31	.74	-25	-22.5
Total 1-20	1.0	1.0	0	100	.26	.58	-17.5	41.3

Full CAM Series

CAM _i /CAM _{TOTAL}					CAM _i /LOD			
Belts	Correlation Lag = 0	Max Correlation	Lag (years) at max Correlation	% Variance Explained	Correlation Lag = 0	Maximum Correlation	Lag (years) at max Correlation	% variance Explained
1	.46	.74	17.5	.8	.27	.35	-7.5	.6
2	.57	.80	15	3.9	.40	.43	-2.5	3.2
3	.65	.84	12.5	5.3	.51	.52	-2.5	5.0
4	.71	.87	7.5	6.1	.61	.61	0.0	6.3
5	.75	.89	7.5	6.5	.69	.69	0.0	7.2
6	.75	.86	7.5	6.6	.75	.75	0.0	7.9
7	.72	.79	5	6.5	.77	.77	0.0	8.3
8	.68	.72	5	6.2	.77	.77	0.0	8.4
9	.63	.65	2.5	5.7	.75	.75	0.0	8.2
10	.58	.59	2.5	5.2	.72	.72	0.0	7.6
11	.55	.55	0.0	4.5	.70	.70	0.0	6.8
12	.55	.55	0.0	3.9	.68	.68	0.0	5.7
13	.58	.58	0.0	3.2	.66	.66	0.0	4.4
14	.64	.64	0.0	2.7	.57	.58	-2.5	2.9
15	.57	.57	0.0	2.3	.25	.52	-10.	1.2
16	.38	.54	-15.	2.2	-.08	.51	-20.	-.6
17	.30	.59	-15.	2.7	-.22	.56	-20.	-2.3
18	.33	.65	-15.	3.9	-.27	.61	-22.5	-3.8
19	.43	.75	-15.	6.6	-.27	.67	-22.5	-4.9
20	.58	.76	-7.5	15.2	-.12	.57	-22.5	-3.7
1-3	.60	.81	15	10.0	.44	.46	-2.5	8.8
4-15	.76	.78	2.5	59.4	.80	.80	0.0	74.9
16-20	.51	.77	-15	30.6	-.21	.67	-22.5	-15.3
Total 1-20	1.0	1.0	0.	100	.57	.64	-5	68.4

Shorter CAM Series

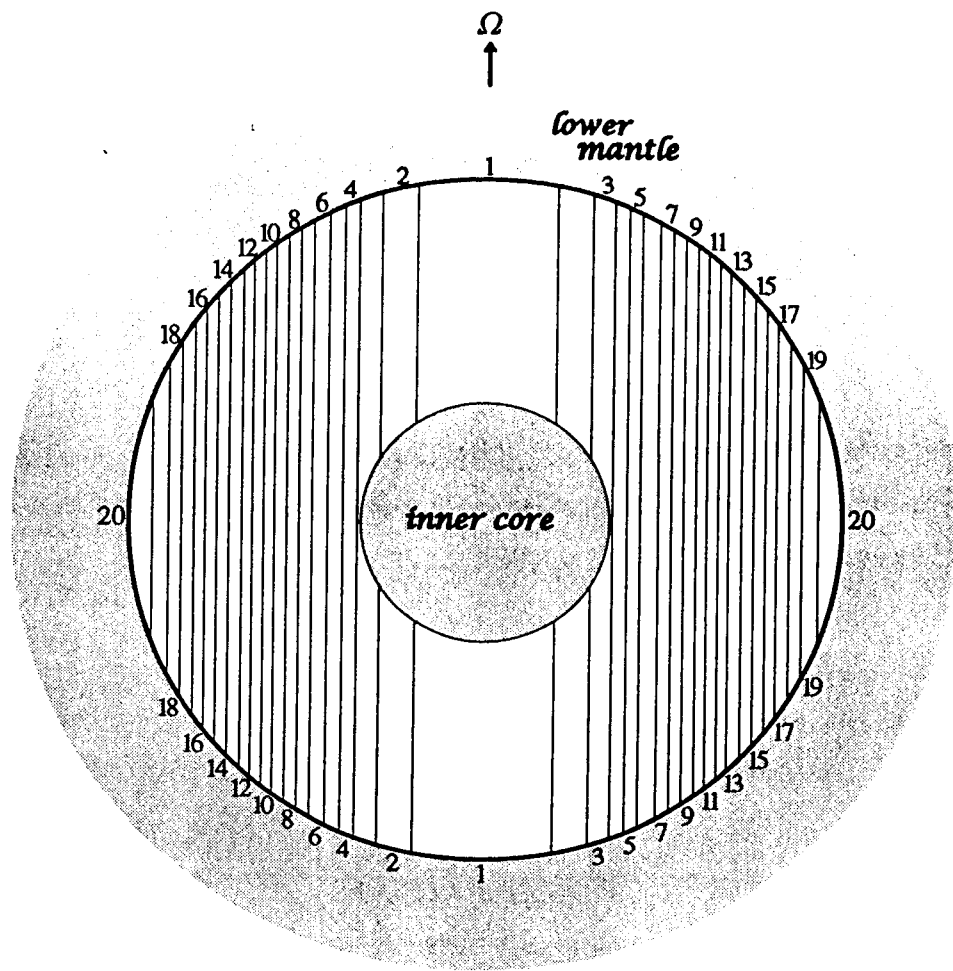


Figure 1

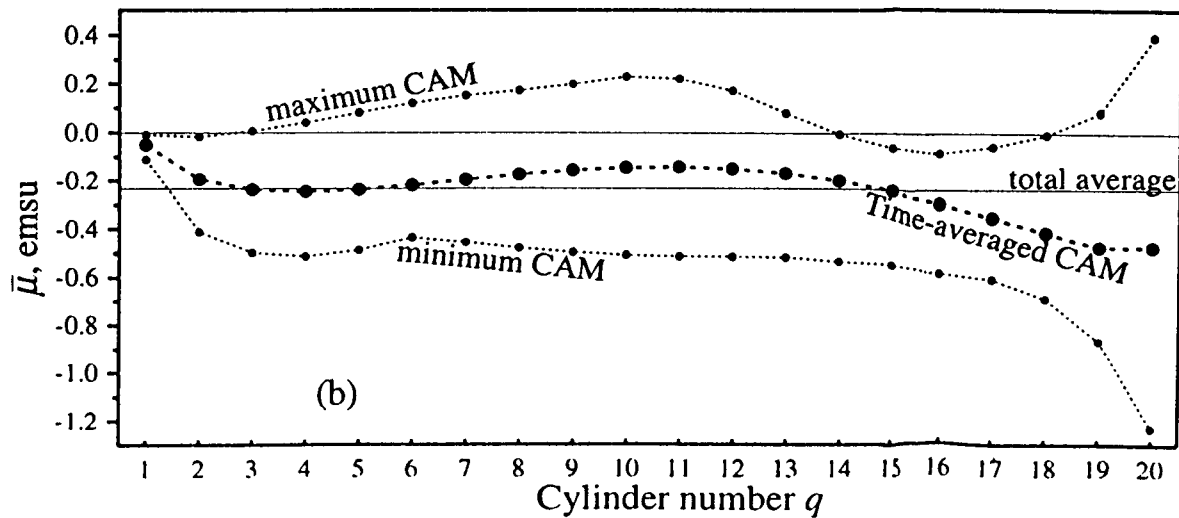
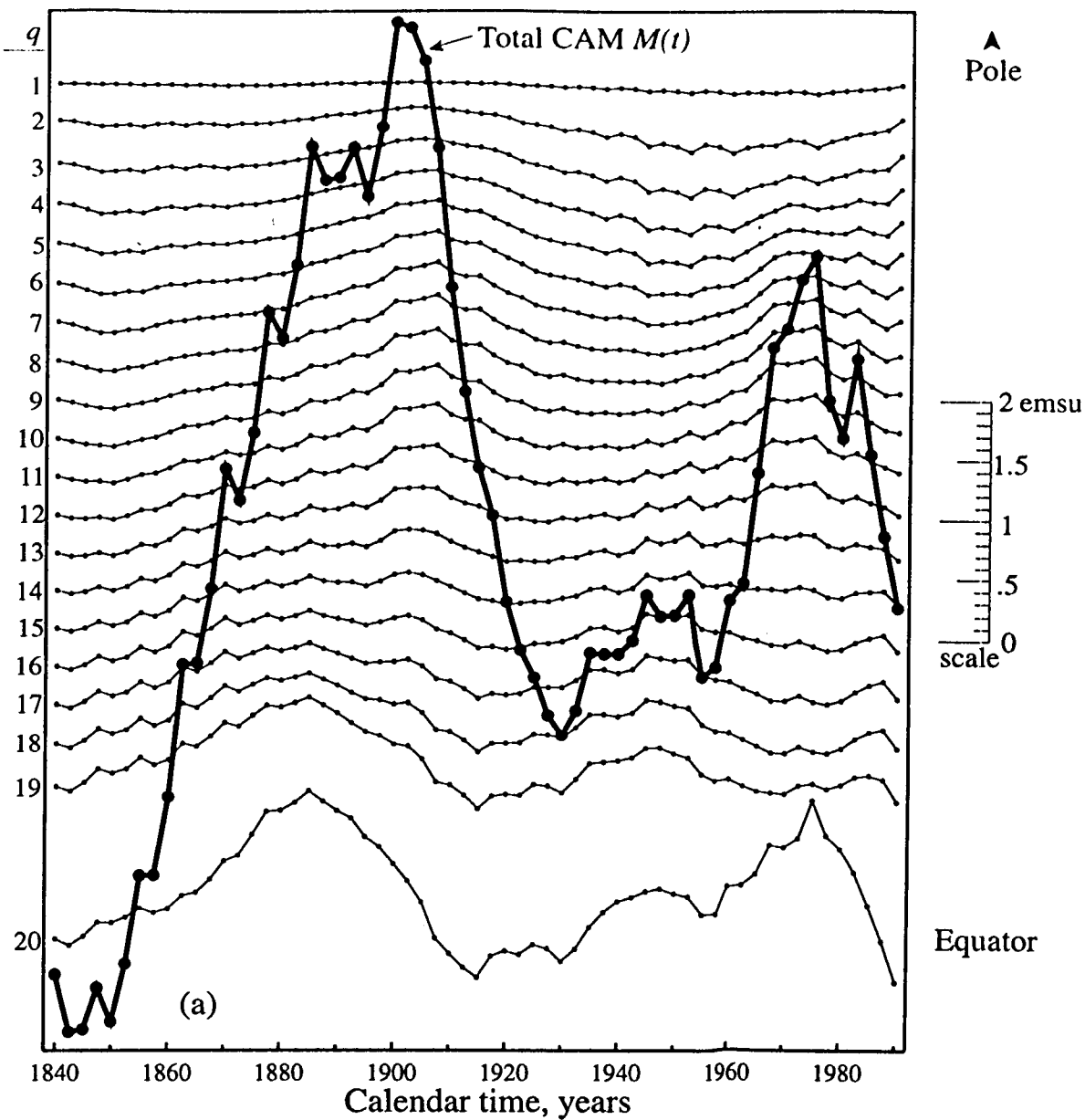


Figure 2

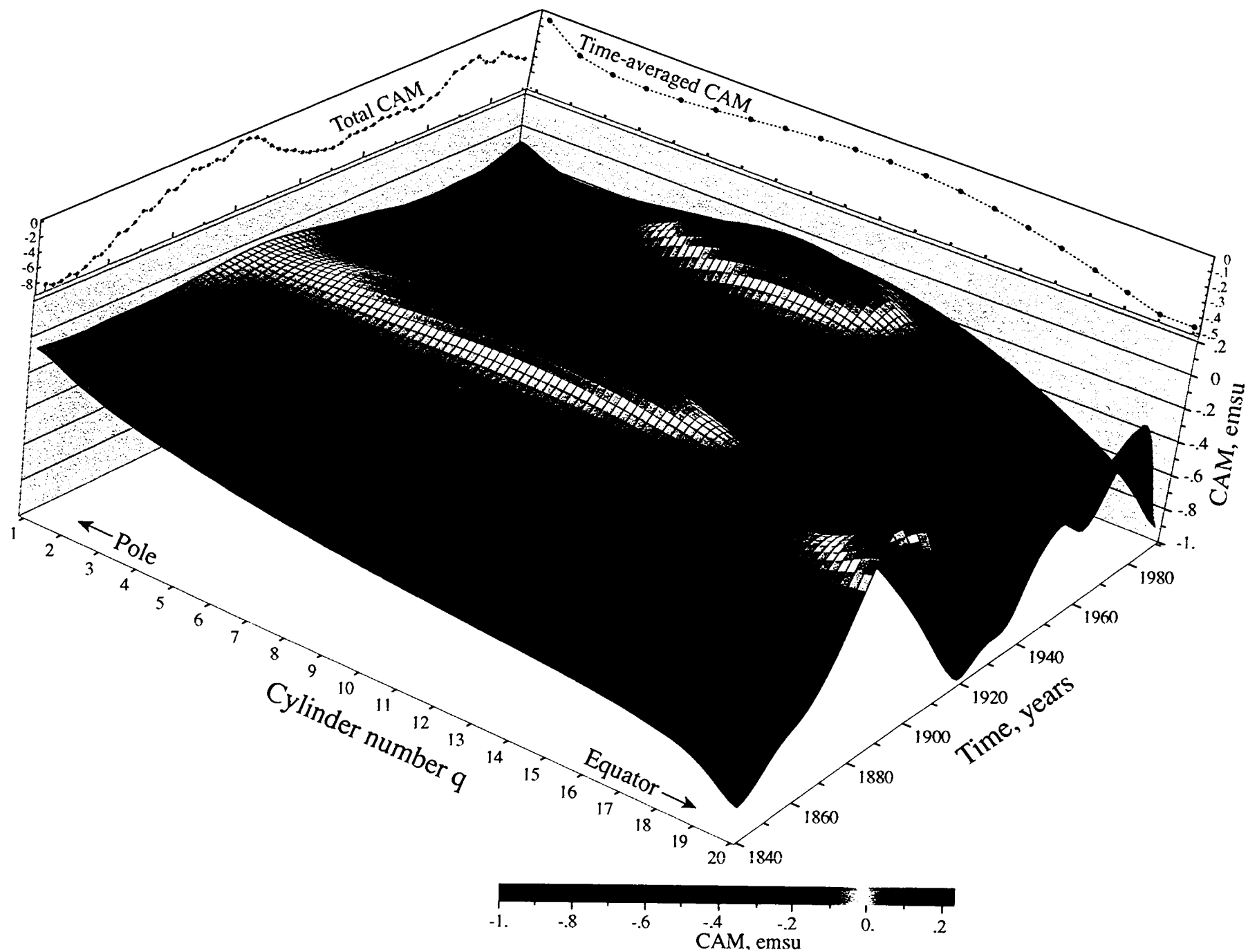


Figure 3(a)

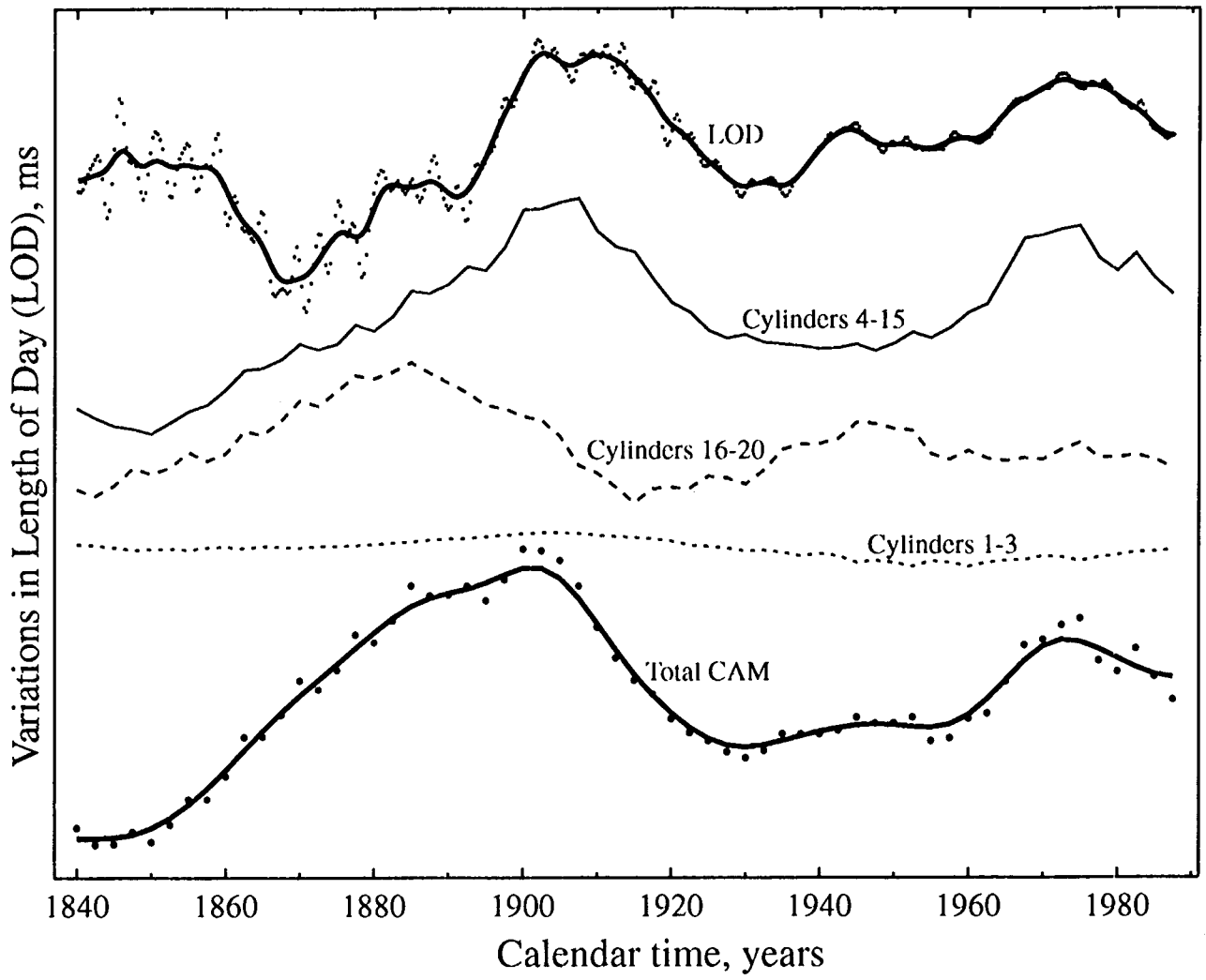


Figure 4

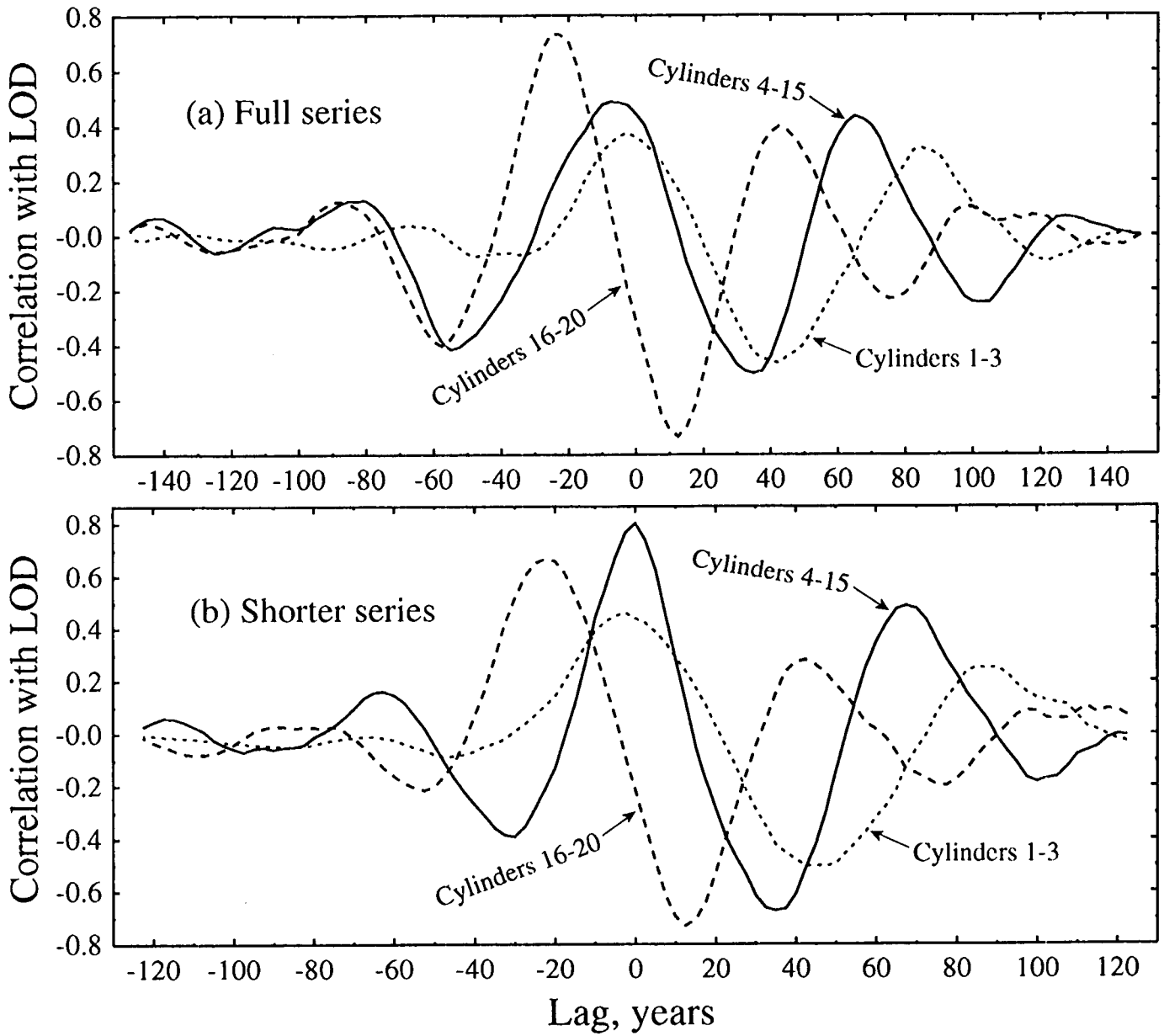


Figure 5

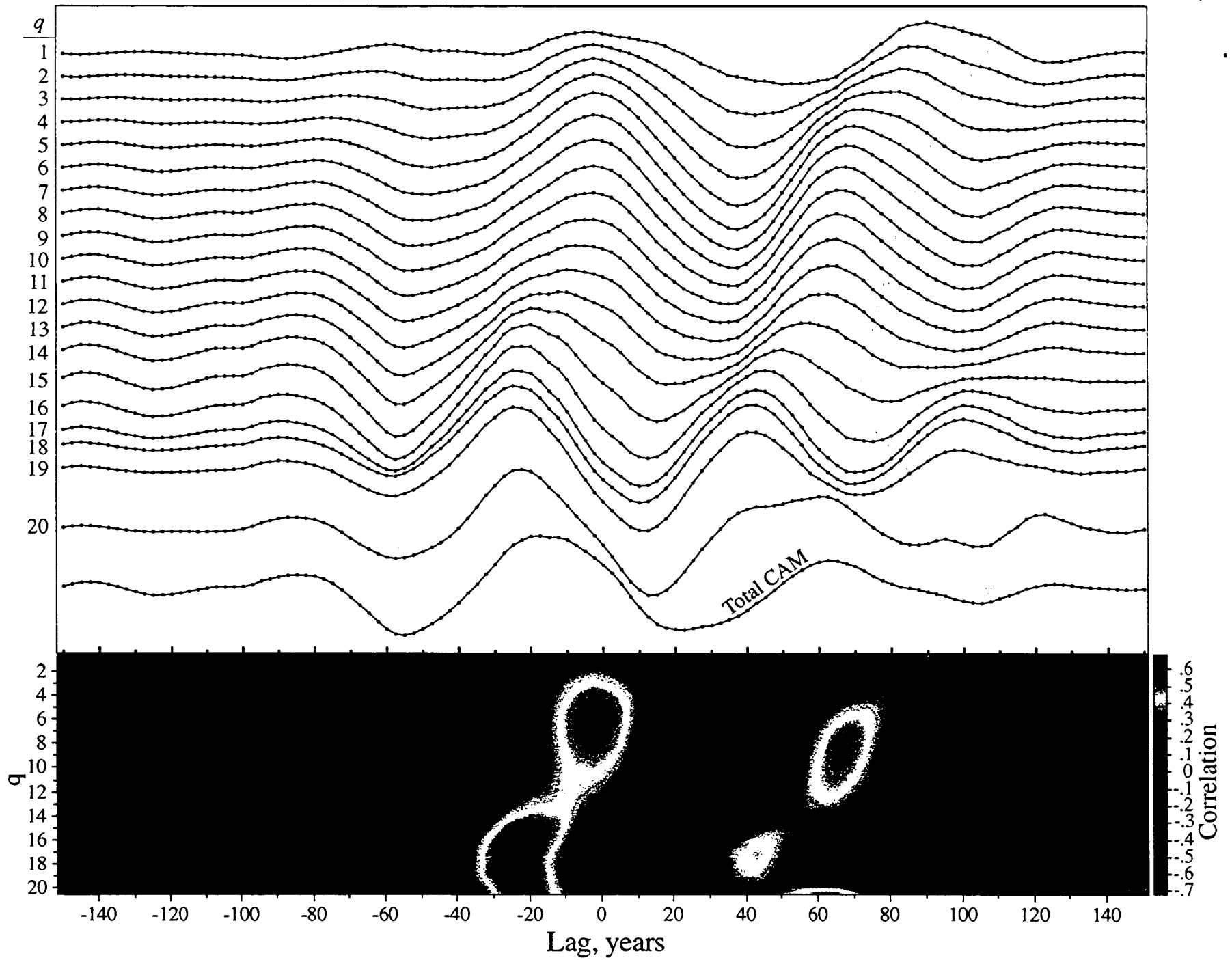


Figure 6